CHEMBIOCHEM

DOI: 10.1002/cbic.200800668

Understanding the Plasticity of the α/β Hydrolase Fold: Lid Swapping on the *Candida antarctica* Lipase B Results in Chimeras with Interesting Biocatalytic Properties

Michael Skjøt,[c] Leonardo De Maria,[c] Robin Chatterjee,[b] Allan Svendsen,[c] Shamkant A. Patkar,[a] Peter R. Østergaard,[a] and Jesper Brask*[a]

The Candida antarctica *lipase B (CALB) has found very extensive use in biocatalysis reactions. Long molecular dynamics simulations of CALB in explicit aqueous solvent confirmed the high mobility of the regions lining the channel that leads into the active site, in particular, of helices α5 and α10. The simulation also confirmed the function of helix α5 as a lid of the lipase. Replacing it with corresponding lid regions from the CALB homologues from* Neurospora crassa *and* Gibberella zeae *resulted in two new CALB mutants. Characterization of these revealed several interesting properties, including increased hydrolytic activity on simple esters, specifically substrates with C_α branching on the carboxylic side, and much increased enantioselectivity in hydrolysis of racemic ethyl 2-phenylpropanoate (E > 50), which is a common structure of the profen drug family.*

Introduction

Candida antarctica lipase B (CALB) has found very extensive use in biocatalysis reactions.[1–3] Applications include both aqueous hydrolysis and nonaqueous acylation reactions; these reactions utilize the enzyme's high activity on a broad range of substrates, which is often combined with outstanding chemo-, regio-, and/or enantioselectivity. Numerous examples from academia and industry illustrate CALB's versatility in asymmetric biocatalysis; typically it is used to generate chiral building blocks by (dynamic) kinetic resolutions or desymmetrizations.[4–6] Substrates in these applications are usually chiral secondary alcohols (or esters thereof) or the isosteric primary amines ($RCHNH_2R'$), but examples also exist with chiral primary alcohols or chiral carboxylic acids (or esters thereof). In the resolution of secondary alcohols, CALB displays Kazlauskas selectivity, that is, the *R* alcohol (or ester thereof) is most often the faster-reacting enantiomer.[7] Further, the impressive activity of CALB in acylation reactions under mild conditions has also been utilized for applications not involving stereochemistry, such as enzymatic polymerizations[8,9] or chemoselective esterifications.[10] Despite its versatility, CALB also has limitations in its accommodation of substrates. Bulkiness, such as branching in the α-position of the carboxylic acid, is problematic, and various functionalized or sterically hindered secondary alcohols[11] and all tertiary alcohols are poor substrates. For such applications, the other lipase from *C. antarctica*, CALA, is often a much better starting point.[12]

Not counting the signal and propeptide sequence (18 + 7 = 25 amino acids), the CALB sequence is 317 aa with the catalytic serine at S105. We have previously reported thermostability, activity, and enantioselectivity for a few single point mutated CALB variants.[13,14] More recently, other groups have also generated and reported CALB variants with improved properties.[15] A group from Schering–Plough used error-prone PCR to produce mutants with increased thermostability[16] and DNA family shuffling to produce other mutants with increased hydrolysis activity toward a prochiral diester substrate.[17] In the latter work homologous lipases from *C. antarctica*, *Hypozyma* sp. and *Crytococcus tsukubaensis* were shuffled. Mutants were also identified with increased thermostability relative to CALB (thermostability close to that of the *Hypozyma* parent). Chodorge et al. used error-prone PCR to generate CALB variants, which were screened for enhanced thermostability.[18] The variant N292Y showed 7.5-fold increased activity after incubation at 90 °C for 15 min. In a series of publications, Hult and co-workers report the effect of rational single point mutations in the CALB active site. With a T40A or T40V substitution, enantioselectivity could be dramatically improved for hydrolysis of ethyl 2-hydroxypropanoate.[19] The authors highlight this as an example of substrate-assisted catalysis. With a S47A mutation, the enantiomeric ratio (*E*) was doubled for acylation of certain racemic secondary alcohols (halohydrins).[20] Similarly, a W104A mutant expanded this pocket and showed increased activity with alcohols such as heptan-4-ol and nonan-5-ol.[21] Interestingly, Hult and co-workers have also investigated aldol and Michael additions,[22–25] and Baeyer–Villiger oxidations[26] with the catalytic serine variant S105A. In a novel approach,

[a] *Dr. S. A. Patkar, Dr. P. R. Østergaard, Dr. J. Brask*
Department of Protein Biochemistry, Novozymes A/S
Krogshoejvej 36, 2880 Bagsvaerd (Denmark)
E-mail: jebk@novozymes.com

[b] *R. Chatterjee*
Present address: Department of Biochemistry at School of Biotechnology
Royal Institute of Technology, Stockholm (Sweden)

[c] *Dr. M. Skjøt,[+] Dr. L. De Maria,[+] Dr. A. Svendsen*
Department of Protein Design, Novozymes A/S

[+] *These authors contributed equally to this work.*

Supporting information for this article is available on the WWW under http://dx.doi.org/10.1002/cbic.200800668.

Lutz and co-workers reported increased catalytic activity of CALB variants produced by circular permutation.[27,28] Variants were identified with increased k_{cat} and k_{cat}/K_M for hydrolysis of 4-nitrophenyl (pNP) butyrate and 6,8-difluoro-4-methylumbelliferyl (DiFMU) octanoate. One variant, cp283, was further immobilized and assayed in nonaqueous esterification and transesterification reactions. This demonstrated in general very similar *E* values for the variant and the wild-type (wt) enzyme. Specifically for esterification of 2-phenylpropanoic acids (profen-like) approximately twofold increased *E* and k_{cat}/K_M values were found.

Here, we describe the design and characterization of novel CALB mutants in which the entire CALB lid region is substituted with that of homologues.

Results and Discussion

The CALB structure — molecular dynamics and alignment

The crystal structure of CALB was solved already in 1994 by Uppenberg et al. as only the sixth lipase structure.[29] It was found that CALB is a globular α/β-type protein composed of seven central β strands that are flanked on both sides by ten α helices. This α/β hydrolase fold was first identified in 1992[30] and has been extensively reviewed in recent years.[31–33] A still-growing number of lipases and esterases are members of this fold. Although the sequence similarity between them is low, their structures share a significant number of secondary elements arranged in similar tertiary structural motifs. As pointed out by Heikinheimo et al., the α/β hydrolase fold is arguably the most plastic of protein folds because it tolerates large insertions into a single-domain protein.[32] Uppenberg et al. found the CALB structure in what appeared to be an "open" conformation with the active site accessible to the solvent, and the short α-helix, α5 (defined as residues 142–146), was pointed out as a putative lid.[29] The long C-terminal α10 (residues 268–287) was hypothesized to play a role in CALB activation and active-site accessibility. In 1995, Uppenberg et al. published the structure of CALB with a covalently bound phosphonate inhibitor.[2] It was then suggested that the α5 helix interacts with the acyl part of a substrate, but does not act as a proper lipase lid. Hence, it was concluded that CALB in fact lacks a lid structure—an issue that has been debated ever since.

In this study, we have addressed the mobility of CALB in aqueous solution. Our molecular dynamics (MD) simulation follows the enzyme over 10 ns, which is four-times longer than previously reported simulations.[34,35] The most striking event that was observed during this investigation is a large motion of the α5 helix towards the C-terminal part of the α10 helix. A representative configuration was extracted from the simulation and is compared with the crystal structure of CALB in Figure 1.

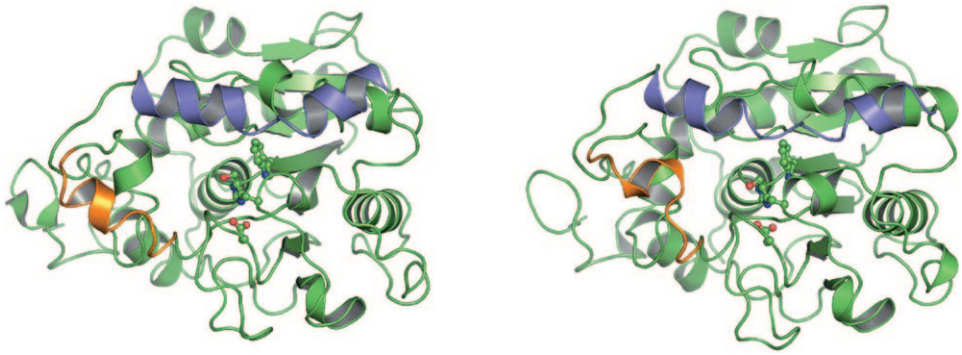

Figure 1. CALB conformations. Left: the crystal structure 1TCA. The α5/α10 helices and flanking regions are shown in orange/blue. The catalytic triad and W104 are shown with sticks and spheres. Right: CALB as obtained from the MD simulation, with the same color code.

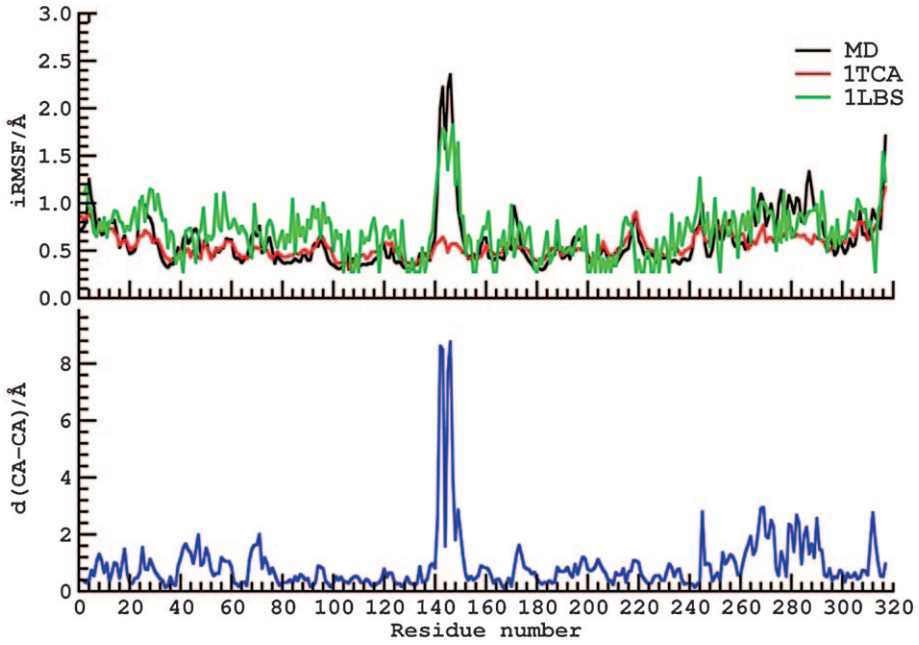

Figure 2. CALB mobility. Upper graph: the Cα isotropic root mean square fluctuations (iRMSF) as obtained from the MD simulation, and two representative crystal structures (PDB ID: 1TCA and 1LBS). Lower graph: the Cα–Cα distance between corresponding residues after optimal superimposition of the CALB structure from Figure 1 (right) onto the crystal structure (1TCA). Regions that are more distant from the crystal structure overlap clearly with the α5/α10 helices and flanking regions.

During this motion D145 becomes fully solvated and loses its interactions with both S150 and T158, and P143 comes in contact with L285 on the C-terminal part of the α10 helix. The displacement of the α5 helix leaves also parts of the α6 helix exposed to the solvent.

The isotropic root mean square fluctuations (iRMSF) for the C_α atoms obtained from the above-mentioned simulation are consistent with those of the monoclinic crystal form of the enzyme (Figure 2, upper panel) as well as with those obtained by Trodler and Pleiss in their recent simulation study.[35] The α5 and α10 helices are the most mobile elements in the polypeptide chain. In Figure 2, lower panel, a detailed comparison of the average configuration that arises from the simulation and the crystal structure used to start it, confirms the mobility data. Taken together with the crystallographic work, our simulation results point to the α5 helix in the CALB structure as a very mobile element that interacts loosely with the rest of the polypeptide chain and consequently is not particularly constrained from a sequence point of view.

This line of thought is confirmed when CALB and homologues are aligned. From regular BlastP searches, six molecules can be identified with >30% identity to CALB: *Ustilago maydis* (Q4PEP1), *Gibberella zeae* (*Fusarium graminearum*) (Q4HUY1), *Debaryomyces hansenii* (Q6BVP4), *Aspergillus fumigatus* (Q4WG73), *Aspergillus oryzae* (Q2UE03) and *Neurospora crassa* (Q7RYD2). We aligned these molecules as well as the previously described CALB homologue from *Hyphozyma* sp.[36] to CALB in their mature forms as determined by SignalP analysis.[37] This clearly indicated a region of high complexity that corresponds to the CALB α5 helix and flanking residues, which span the residues from 135 to 155 (Figure 3). Marked differences in lid regions have previously also been observed among pancreatic lipases.[38]

Lid swapping-design, cloning, expression and purification

In their work with circular permutation, Qian and Lutz recently identified the α5 helix of CALB as a region where backbone cleavage could be allowed (leading to functional molecules), but the tested variants did not show significantly improved activity in hydrolysis of pNP butyrate and DiFMU octanoate.[27] The above-mentioned results from MD simulations and the alignment, however, prompted us to further investigate the role of this region. We accordingly embarked on a project of generating CALB variants with this region substituted with the corresponding regions from the homologues. A similar strategy of "lid swapping" has previously been explored by Secundo, Jaeger and co-workers, who mainly worked with *Candida rugosa* lipase isoenzymes, but they also investigated lid mutations in the *Pseudomonas fragi* lipase, as well as insertion of lid fragments from homologues on the lid-less *Bacillus subtilis* lipase A.[39] In our work with CALB, in particular the transfer of lids from the *N. crassa* and *G. zeae* homologues resulted in chimeric lipases with interesting properties. These enzymes were "CALB-*N. crassa*" (with a lid from Q7RYD2): Y135F, K136H, V139M, G142Y, P143G, D145C, L147G, A148N, V149F, S150G, KVAKAGAPC, A151P, W155L, and "CALB-*G. zeae*" (with a lid from Q4HUY1): V139I, G142N, P143I, L144G, D145G, L147T, A148G, V149L, S150IN, A151T, S153A, W155V. Variants were made by splicing by overlapping extension PCR (SOE-PCR)[40] followed by sequence confirmation of the resulting variants. The inserted regions were designed to be encoded by optimal *Aspergillus* codon usage, and the resulting fragments were cloned into an *Aspergillus* expression vector and expressed from recombinant *Aspergillus* essentially as described by Huge-Jensen and co-workers.[41] Following filtration of the culture broth, the variants were chromatographically purified and their identity was confirmed by N-terminal sequencing.

Characterization of CALB-*N. crassa* and CALB-*G. zeae*

Initially, for kinetic characterization of these two CALB variants in comparison to the CALB wt enzyme, hydrolysis assays based on the pNP esters of butyric acid (**1**), (*R*,*S*)-2-methylbutyric acid (**2**) and lauric acid (**3**) were conducted (Scheme 1). Whereas **1** is the standard substrate of choice, the other two structures were included to investigate how the variants accommodate carboxylic C_α branching and longer acyl chains. This focus was based on the earlier observations by Uppenberg et al. that the α5 helix interacts with the acyl part of the substrate.[2,29] Michaelis–Menten constants of the two variants and the wt enzyme are shown in Table 1. The assays were performed in sodium phosphate buffer (0.5 M, pH 7.0) that contained Triton X-100 (1%) to avoid turbid solutions at high substrate con-

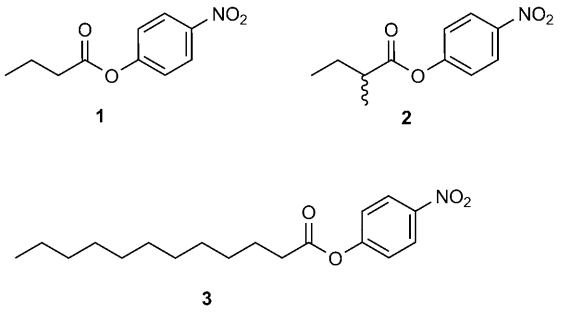

Scheme 1. Structures of pNP substrates.

Table 1. Kinetic constants and enantiomeric ratio for hydrolysis of pNP esters.

Substrate	Enzyme	k_{cat} [s^{-1}]	K_M [μM]	k_{cat}/K_M [s^{-1} M^{-1}]	*E*
	CALB wt	16±1	484±11	33000	n.a.
1	CALB-*N. crassa*	39±11	250±12	160000	n.a.
	CALB-*G. zeae*	8±2	169±32	47000	n.a.
	CALB wt	0.09±0.02	525±99	170	1.05±0.02
2	CALB-*N. crassa*	1.2±0.2	318±24	3900	2.4±0.2
	CALB-*G. zeae*	0.30±0.03	335±111	900	1.08±0.02
	CALB wt	3.1±0.3	535±32	5800	n.a.
3	CALB-*N. crassa*	2±1	450±251	4400	n.a.
	CALB-*G. zeae*	23±6	170±15	140000	n.a.

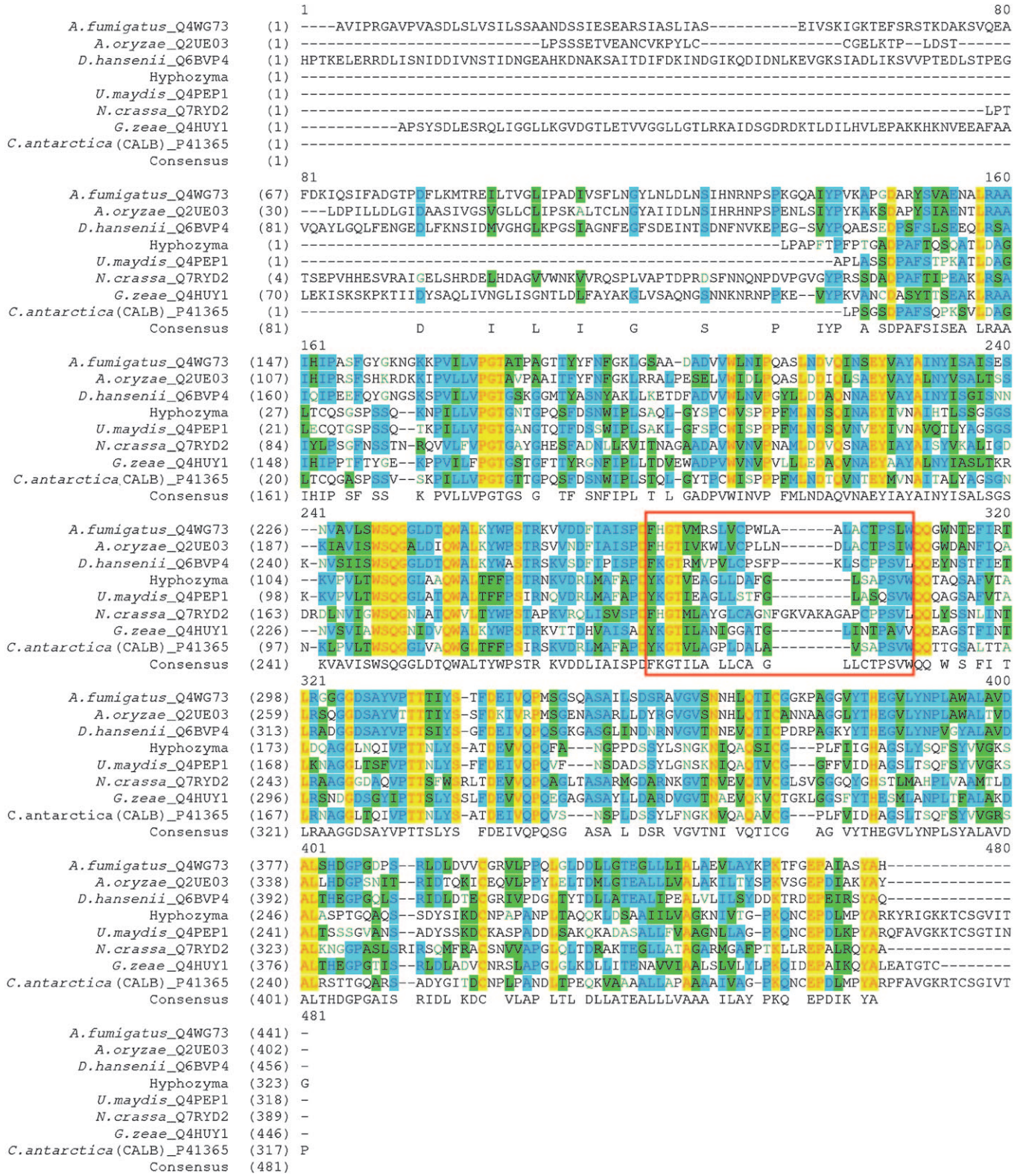

Figure 3. Alignment of CALB homologues. Black on white: dissimilar residues. Blue on cyan: consensus residues derived from a block of similar residues at a given position. Black on green: consensus residues derived from the occurrence of greater than 50% of a single residue at a given position. Red on yellow: consensus residues derived from a completely conserved residue at a given position. Green on white: residues weakly similar to consensus residues at a given position. The region of high complexity targeted for replacement in CALB is boxed.

centrations. The enantiomeric ratio (*E*) could be calculated for hydrolysis of substrate **2** by acidification of the reaction mixture, followed by extraction into diethyl ether and analysis of the 2-methylbutyric acid product by chiral GC.

Our results indicate that under the stated conditions, the CALB-*N. crassa* mutant had a five-times higher k_{cat}/K_M ratio compared to the wt lipase when assayed with pNP butyrate (**1**), and a 23-times higher k_{cat}/K_M ratio with the branched substrate **2**; however, with the longer substrate **3**, CALB-*N. crassa* performed much like the wt, whereas CALB-*G. zeae* had a 24-times higher k_{cat}/K_M ratio. Both the wt enzyme and CALB-*G. zeae* were almost completely unselective towards substrate **2**, but CALB-*N. crassa* did show very modest enantioselectivity ($E = 2.4$). For comparison, Gaub et al. recently reported $k_{cat} = 32\ s^{-1}$ and $K_M = 4612\ \mu M$ for hydrolysis of **1** in phosphate buffer (50 mM, pH 7.0), NaCl (150 mM), Triton X-100 (0.5%), *i*PrOH (5%) by CALB expressed in *Aspergillus*.[42] In the same publication the authors reported very similar kinetic constants for CALB expressed in *E. coli*. Qian and Lutz reported $k_{cat} = 5\ s^{-1}$ and $K_M = 410\ \mu M$ for CALB wt with the same substrate in a pH 7.5 buffer (Triton or cosolvents were not mentioned).[27]

Whereas pNP esters are frequently used for assaying enzyme activity, these activated esters are both electronically and sterically significantly different from the simple alkyl esters that are typically of interest in biocatalytic reactions. To address this issue, a second assay was designed with hydrolysis of a small but diverse set of eight simple esters substrates (Scheme 2). Initially a range of additives and cosolvents were evaluated for their ability to emulsify or dissolve the substrates, and hence increase accessibility for the enzyme. Two conditions were found to be favorable for all substrates, 1) 0.1% Triton X-100 and 2) 5% acetone, both in 50 mM Tris buffer pH 7.0. Reactions were then performed in Eppendorf tubes at 30 °C over 24 h, after which a sample was withdrawn for GC analysis, which was used to calculate both conversion and enantiomeric ratio.

This simple assay revealed several interesting results (Table 2). The most striking was the remarkably improved enantioselectivity for hydrolysis of ethyl (*R,S*)-2-phenylpropanoate (**7**). The wt enzyme showed no enantioselectivity with this substrate at all; this is also described in the literature.[43] In contrast, both mutants hydrolyzed the substrate with excellent enantioselectivity (it has not been investigated if the selectivity is *R* or *S*). Because 2-arylpropanoic acid is a common core structure of the profen drug family (ibuprofen, ketoprofen, etc.), there is significant interest in finding such selective enzymes to facilitate resolution of the racemic drugs or intermediates.[44,45] Both variants also showed increased activity with the difficult C_α-branched ethyl (*R,S*)-2-ethylhexanoate (**5**), with which the wt enzyme had no detectable activity. Further, with this substrate, enantioselectivity was excellent ($E > 50$) for both variants, and interestingly, conversion was higher with 0.1% Triton X-100 compared to 5% acetone (for all other reactions the two media gave very similar results).

Table 2. Conversion (%) and enantiomeric ratio (E)[a] after 24 h reaction for the systems with either Triton X-100 (0.1%) or acetone (5%).

Substrate	Condition	CALB wt	CALB-*N. crassa*	CALB-*G. zeae*
4	Triton	92 (1.1)	99 (1.0)	97 (1.0)
	acetone	92 (1.1)	98 (1.0)	97 (1.1)
5	Triton	0	24 (>50)	26 (>50)
	acetone	0	7 (>50)	4 (>50)
6	Triton	30	30	24
	acetone	36	38	27
7	Triton	41 (1.0)	24 (>50)	30 (23)
	acetone	44 (1.3)	24 (>50)	23 (>50)
8	Triton	97	96	96
	acetone	97	94	97
9	Triton	38 (>50)	47 (>50)	46 (>50)
	acetone	42 (>50)	38 (>50)	40 (>50)
10	Triton	93	73	79
	acetone	86	75	67
11	Triton	58 (3.9)	53 (5.1)	40 (15)
	acetone	40 (12)	49 (5.5)	33 (14)

[a] $E > 50$ means that only one enantiomer could be detected by the standard GC analysis. The same amount of enzyme (0.5 mg) was used in all reactions.

The two mutant enzymes were further characterized and compared by measuring the denaturation temperature (T_d) by differential scanning calorimetry (DSC), and specific activity in the hydrolysis of tributyrin at pH 7 (the "LU assay").[46] For the wt enzyme we found a T_d of 62 °C, which confirms previously published data.[14] The two mutants showed little variation relative to the wt denaturation temperature: the T_d values were determined to be 60 and 63 °C for CALB-*N. crassa* and CALB-*G. zeae*, respectively. For comparison, Lutz and co-workers determined T_M for CALB wt to be 53.5 °C by fitting thermal denaturation CD spectroscopy data, with the circular permutated variants giving significantly reduced T_M values.[28] When we measured the specific activity with the LU assay, CALB wt gave a familiar bell-shaped pH profile with a optimal specific activity at pH 7, which is close to what we have previously reported (Figure 4).[14] The two variants, on the other hand, yielded surprisingly low specific activities in this assay. Furthermore, the pH profiles were entirely different: there was no clear optimum, but a tendency to higher activity under more alkaline

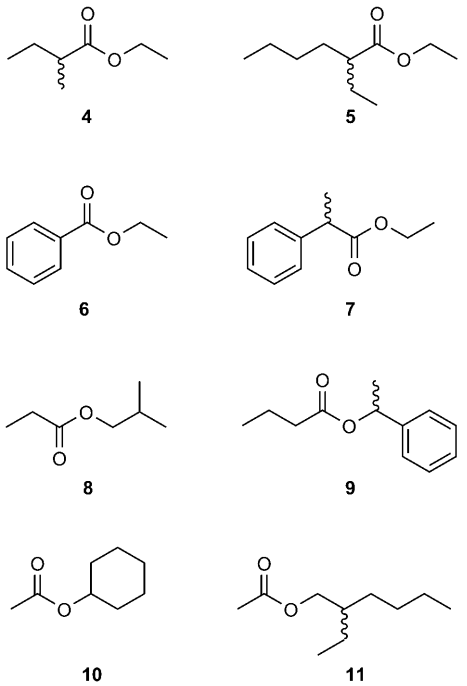

Scheme 2. Structures of ester substrates used for hydrolysis assay.

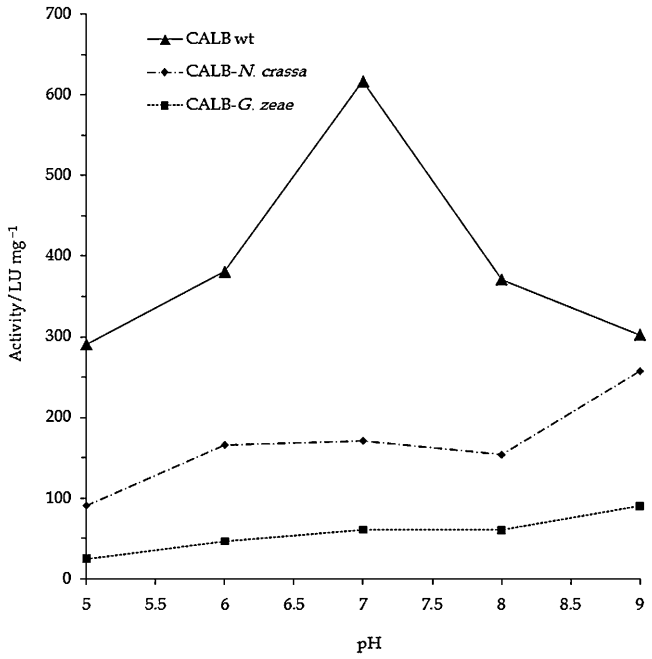

Figure 4. The pH profiles of the enzymes studied in the LU assay.

conditions. Whether the poorer performance of the variants in this assay is due to the triglyceride substrate structure or other reaction conditions, is not certain.

Finally, to investigate the performance of the two mutants in acylation reactions under nonaqueous conditions, the enzymes were immobilized on porous polypropylene beads. The enantioselectivity was then evaluated for acylation of a racemic secondary (hexan-3-ol; **12**) and primary (2-ethylhexan-1-ol; **13**) alcohol in hexane by using vinyl acetate or propionate as acyl donors (Scheme 3). With the secondary alcohol **12**, both wt and the two variants showed excellent enantioselectivity ($E >$ 50), but the primary alcohol **13** gave poor enantioselectivity, although it was slightly improved in the variants compared to the wt (Table 3). Reaction rates were similar for the three enzymes, though the two variants appeared slightly slower than the wt in acylation of substrate **13**. The increase in enantioselectivity for acylation of **13** is small but significant, and indicates that the lid plays a role in dictating the selectivity in apolar nonaqueous media too.

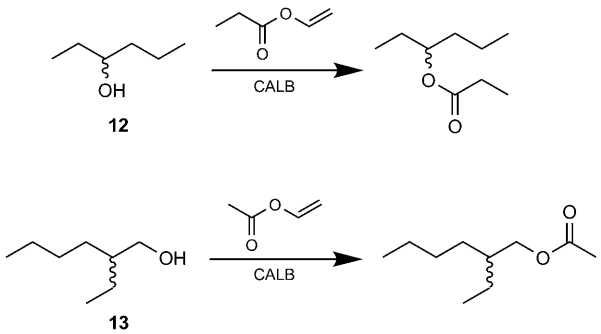

Scheme 3. Transesterification reactions catalyzed by immobilized CALB.

Table 3. Enantiomeric ratio (E) determined from nonaqueous transesterification reactions with alcohols **12** and **13**.

	12	13
CALB wt	>50	1.9
CALB-*N. crassa*	>50	3.0
CALB-*G. zeae*	>50	3.2

Conclusions

Historically, the significance and even presence of a CALB lid has been debated, though the α5 and α10 helices originally were suggested as lid candidates. We have now been able to establish with MD simulations that α5 and α10 are in fact highly mobile regions in the CALB structure, and also exhibit a relative motion between them. The simulations presented in this work also point at the α5 helix and its flanking residues as loose regions that have few physical contacts with the rest of the molecule. This was further confirmed by sequence alignments in which this residue stretch was found to have remarkable low similarity in seven CALB homologues. To investigate the role of this region, mutant lipases were created in which this sequence of the wt CALB was replaced with that of the homologues from the alignment. We succeeded in expressing several of these molecules in *Aspergillus*, and from this handful, two were initially selected to be studied further, based on high activity measured with a simple pNP butyrate assay directly in the fermentation broth. These were CALB-*N. crassa*, which had a very large lid, and CALB-*G. zeae*, which had a much smaller lid structure. The biocatalytic screening of these two mutants revealed several interesting properties, including increased hydrolytic activity with a range of ester substrates, in particular those with C_α branching on the carboxylate, as well as much increased enantioselectivity in hydrolysis of a 2-arylpropanoic acid ester. From an application point of view, this positions CALB-*N. crassa* and CALB-*G. zeae* as two potentially very interesting enzymes for a range of biocatalytic reactions. The results also illustrate that the CALB sequence stretch around the α5 helix can indeed significantly influence the catalytic properties of the enzyme, including the enantioselectivity, which consequently seems not only to be dictated by the fit of the substrate into the enzyme's active site pocket. Finally, this work provides evidence in support of the high plasticity of the α/β hydrolase fold, and shows how entire regions of the polypeptide chain that are loosely bound to the rest of the protein matrix can be completely interchanged.

Experimental Section

Molecular dynamics and alignment: CHARMm® was used to prepare the CALB (PDB ID: 1TCA) structure for the simulations, as described in previous studies.[34,35] D134 was neutralized by adding a proton to ensure a neutral enzyme at neutral pH values. Hydrogen

atoms were added to both protein and waters by using the command HBUILD. The system was embedded in explicit water molecules and confined to a 90 Å cubic box. There were in total 24630 water molecules, including those that were already present in the 1TCA structure. A simulation at constant temperature (300 K) and constant pressure (102668 Pa) was performed for a total of 10 ns by using NAMD.[47] Berendsen's coupling method[48] was used to keep the temperature and the pressure at the desired values. The temperature coupling constant was set to 0.25 ps^{-1} and the compressibility parameter for the barostat was set to 4.55×10^{-5} bar^{-1}. Hydrogen atoms were constrained by the SHAKE algorithm by allowing for a 2 fs time step.[49] Long-range interactions were switched from 8 to 12 Å, at which point they were cut off. More details about the simulation can be found in the Supporting Information. The alignment was done by using the AlignX program from the Vector NTI package (Invitrogen) version 10.3.0 by using standard parameters.

Cloning and expression: CALB variants were created by SOE-PCR by using a vector that harbored the wt CALB coding region as template for the primary PCR. Insertion of Q7RYD2 lid: PCR-A: primer 387: 5′-TGG CGA CCT TGC CGA AGT TGC CGG CGC AGA GGC CGT AGG CGA GCA TGG TGC CGT GGA AGT CGG GCG CAA AGG CCA TAA GTC GAT C-3′ + primer 399: 5′-CCG GTG ACC CTC GAG ACC ATG AAG CTA CTC TCT CTG ACC-3′ and PCR-B: primer 388: 5′-TCT GCG CCG GCA ACT TCG GCA AGG TCG CCA AGG CCG GCG CCC CCT GCC CCC CCT CCG TCC TCC AGC AAA CCA CCG GTT CGG CAC TCA CC-3′ + primer 400: 5′-TCA CCC TCT AGA TCT TCA GGG GGT GAC GAT GCC GG-3′. Insertion of Q4HUY1 lid: PCR-C: primer 398: 5′-GCC AAC ATC GGC GGC GCC ACC GGC CTC ATC AAC ACC CCC GCC GTC GTC CAG CAA ACC ACC GGT TCG GCA CTC ACC-3′ + primer 400 and PCR-D: primer 387 + primer 399. The resulting fragments were gel purified and small aliquots of PCR-A + B and PCR-C + D were mixed and used as templates for the generation of the Q7RYD2 and Q4HUY1 lid mutants, respectively, by using primers 399 and 400 for the secondary amplification. The Phusion™ High-Fidelity DNA Polymerase (Finnzymes) was used as described by the manufacturer for all amplifications. Primers 399 and 400 introduced BglII/XhoI In-Fusion (Clontech Laboratories, Inc.) capable overhangs. The vector pENI1898Link, which contained the TAKA promoter and a downstream AMG terminator that enabled the expression of the variants in *Aspergillus*,[50] was digested with BglII/XhoI, and the final amplification products were introduced by In-Fusion™ PCR cloning. The two variants were sequenced by using a ABI 373 DNA sequencer (Applied Biosystems) to confirm that only the desired mutations were introduced. The two resulting plasmids were transformed into *A. oryzae* as previously described.[41] A selection of transformants were grown in YPM (10 g yeast extract (Difco), 20 g peptone (Difco), water to 1 L, autoclaved; added sterile-filtered maltose to 2%, *w*/*w*) for four days at 30 °C with vigorous shaking, prior to purification of the variants.

Purification: The culture broth was first filtered though filtration cloth and subsequently through a 0.2 μm filtration unit (Nalgene) to remove the *Aspergillus* host. Solid NaCl was added to 1 M final concentration and the pH was adjusted to 7 with AcOH (20%). The adjusted lipase solution was applied to a decyl-agarose column (prepared by immobilizing decyl groups on activated agarose) and equilibrated in 50 mM HEPES/NaOH, NaCl (1.0 M), pH 7.0. After washing the column with the equilibration buffer, the column was eluted with 50 mM HEPES/NaOH, pH 7.0. The eluted peak, which containing the lipase, was dialyzed, overnight, in 20 mM AcOH/NaOH, pH 4.5 and applied to a SOURCE S column (GE Healthcare) that had been equilibrated in 20 mM AcOH/NaOH, pH 4.5. The column was washed with the equilibration buffer and eluted with a linear NaCl gradient (0 to 0.5 M) over ten column volumes. The lipase, which eluted as a sharp peak was collected, and the purity was analyzed by SDS-PAGE; only one band was found on the Coomassie-stained gel. Finally, N-terminal sequencing was performed by Edman degradation by using an Applied Biosystems 494 Procise system, by following standard procedures recommended by the manufacturer.

DSC and pH profile: Denaturation temperatures (T_d) were determined by using a MicroCal VP-DSC instrument in HEPES buffer (50 mM, pH 7) with approximately 1 mg mL^{-1} enzyme concentration. The scan range was 20–90 °C at 90 °C h^{-1}. The pH profiles were based on LU activity measurements. The LU assay is a pH-stat-based titration of the enzymatic hydrolysis of tributyrin (0.17 M) emulsified with gum Arabic (0.1%), as previously described.[46]

Determination of Michaelis–Menten constants: The pNP substrates were dissolved in propan-2-ol to make a 100 mM stock solution. This was added to sodium phosphate buffer (0.5 M, pH 7.0) with Triton X-100 (1%) to obtain substrate concentrations in the range 0.01–2 mM (high concentrations were not possible for pNP laurate). Next, the substrate solutions (150 μL) was transferred to a a microtiter plate, and enzyme (10 μL) was added. Absorption was measured at 405 nm every 15 s over 20 min. Reaction rates (A_{405} s^{-1}) were converted to M s^{-1} by using an experimentally determined pNP standard curve (in the given buffer) and the data were plotted against substrate concentration. Next, v_{max} and K_M were calculated from a direct fit to the Michaelis–Menten plot by using the solve function in MS Excel. Finally, v_{max} was converted to k_{cat} by dividing with enzyme concentration, which was calculated from measured A_{280} by using a theoretical molar extinction coefficient that was calculated with GPMAW (http://www.gpmaw.com). The given standard deviations refer to k_{cat} and K_M calculations from three different batches of each of the three enzymes (individual fermentations and purifications).

Determination of *E* for pNP 2-methylbutyrate hydrolysis: Reactions were performed on the 2 mL scale by using 2 mM substrate and the same buffer system as for the determination of the kinetic constants. Three reactions were stopped by the addition of HCl (2 M, 0.1 mL) and then extracted into Et_2O (2 mL). After analysis by chiral GC (Varian CP-Chiralsil-DEX CB 10 m column, temperature program 80 to 180 °C at 2 °C min^{-1}), *E* was calculated from Equation (1):

$$E = \frac{\ln[ee_p(1-ee_s)/(ee_p+ee_s)]}{\ln[ee_p(1+ee_s)/(ee_p+ee_s)]} \quad (1)$$

Reactions were performed in triplet for each enzyme (stopped at different conversions) and *E* is reported as an average.

Hydrolysis reactions with simple ester substrates: Reactions were performed with substrate (50 μL) in Tris buffer (50 mM, pH 7.0) that contained either Triton X-100 (0.1%) or acetone (5%). Enzyme (0.5 mg, calculated based on A_{280}) was added and the reaction was incubated for 24 h at 30 °C, 1200 rpm; the total volume was 1.5 mL. To stop the reactions, HCl (1 M, 0.1 mL) was added and the mixture was extracted with CH_2Cl_2 (0.9 mL). The organic phase (20 μL) was transferred to a GC vial that contained Et_2O (980 μL). GC analysis and calculation of *E* was performed as described above. Conversion was calculated directly from the GC integrals without the use of standards.

Immobilizations and nonaqueous reactions: Enzymes were immobilized on Accurel MP1000 porous polypropylene beads by physical adsorption (loading 20 mg g^{-1}, based on A_{280}). After 18 h of shaking at room temperature in phosphate buffer (1 M, pH 7) no residual enzyme was found in the supernatant, and the beads that contained the immobilized enzyme were filtered and dried. Acylation reactions were performed in Eppendorf tubes with each reagent (1 mmol), hexane (0.8 mL) and immobilized enzyme (5 mg) at 40 °C, 1400 rpm. Samples were withdrawn for analysis by NMR spectroscopy (conversion) and chiral GC at specific time intervals. The *E* value was calculated as previously specified.

Keywords: enantioselectivity · enzyme catalysis · ester hydrolysis · gene expression · molecular dynamics

[1] S. A. Patkar, F. Bjorking, M. Zundel, M. Schulein, A. Svendsen, H. P. Heldthansen, E. Gormsen, *Indian J. Chem. Sect. B* **1993**, *32*, 76–80.
[2] J. Uppenberg, N. Ohrner, M. Norin, K. Hult, G. J. Kleywegt, S. Patkar, V. Waagen, T. Anthonsen, T. A. Jones, *Biochemistry* **1995**, *34*, 16838–16851.
[3] E. M. Anderson, M. Karin, O. Kirk, *Biocatal. Biotransform.* **1998**, *16*, 181–204.
[4] A. Ghanem, *Tetrahedron* **2007**, *63*, 1721–1754.
[5] V. Gotor-Fernández, R. Brieva, V. Gotor, *J. Mol. Catal. B: Enzym.* **2006**, *40*, 111–120.
[6] V. Gotor-Fernández, E. Busto, V. Gotor, *Adv. Synth. Catal.* **2006**, *348*, 797–812.
[7] R. J. Kazlauskas, A. N. E. Weissfloch, A. T. Rappaport, L. A. Cuccia, *J. Org. Chem.* **1991**, *56*, 2656–2665.
[8] R. A. Gross, A. Kumar, B. Kalra, *Chem. Rev.* **2001**, *101*, 2097–2124.
[9] S. Kobayashi, H. Uyama, S. Kimura, *Chem. Rev.* **2001**, *101*, 3793–3818.
[10] K. Adelhorst, F. Bjorkling, S. E. Godtfredsen, O. Kirk, *Synthesis* **1990**, 112–115.
[11] M. From, P. Adlercreutz, B. Mattiasson, *Biotechnol. Lett.* **1997**, *19*, 315–317.
[12] P. D. de Maria, C. Carboni-Oerlemans, B. Tuin, G. Bargeman, A. van der Meer, R. van Gemert, *J. Mol. Catal. B: Enzym.* **2005**, *37*, 36–46.
[13] S. A. Patkar, A. Svendsen, O. Kirk, I. G. Clausen, K. Borch, *J. Mol. Catal. B* **1997**, *3*, 51–54.
[14] S. Patkar, J. Vind, E. Kelstrup, M. W. Christensen, A. Svendsen, K. Borch, O. Kirk, *Chem. Phys. Lipids* **1998**, *93*, 95–101.
[15] S. Lutz, *Tetrahedron: Asymmetry* **2004**, *15*, 2743–2748.
[16] N. Y. Zhang, W. C. Suen, W. Windsor, L. Xiao, V. Madison, A. Zaks, *Protein Eng. Des. Sel.* **2003**, *16*, 599–605.
[17] W. C. Suen, N. Y. Zhang, L. Xiao, V. Madison, A. Zaks, *Protein Eng. Des. Sel.* **2004**, *17*, 133–140.
[18] M. Chodorge, L. Fourage, C. Ullmann, V. Duvivier, J. M. Masson, F. Lefevre, *Adv. Synth. Catal.* **2005**, *347*, 1022–1026.
[19] A. Magnusson, K. Hult, M. Holmquist, *J. Am. Chem. Soc.* **2001**, *123*, 4354–4355.
[20] D. Rotticci, J. C. Rotticci-Mulder, S. Denman, T. Norin, K. Hult, *ChemBioChem* **2001**, *2*, 766–770.
[21] A. O. Magnusson, J. C. Rotticci-Mulder, A. Santagostino, K. Hult, *ChemBioChem* **2005**, *6*, 1051–1056.
[22] C. Branneby, P. Carlqvist, K. Hult, T. Brinck, P. Berglund, *J. Mol. Catal. B* **2004**, *31*, 123–128.
[23] C. Branneby, P. Carlqvist, A. Magnusson, K. Hult, T. Brinck, P. Berglund, *J. Am. Chem. Soc.* **2003**, *125*, 874–875.
[24] P. Carlqvist, M. Svedendahl, C. Branneby, K. Hult, T. Brinck, P. Berglund, *ChemBioChem* **2005**, *6*, 331–336.
[25] M. Svedendahl, K. Hult, P. Berglund, *J. Am. Chem. Soc.* **2005**, *127*, 17988–17989.
[26] P. Carlqvist, R. Eklund, K. Hult, T. Brinck, *J. Mol. Model.* **2003**, *9*, 164–171.
[27] Z. Qian S. Lutz, *J. Am. Chem. Soc.* **2005**, *127*, 13466–13467.
[28] Z. Qian, C. J. Fields, S. Lutz, *ChemBioChem* **2007**, *8*, 1989–1996.
[29] J. Uppenberg, M. T. Hansen, S. Patkar, T. A. Jones, *Structure* **1994**, *2*, 293–308.
[30] D. L. Ollis, E. Cheah, M. Cygler, B. Dijkstra, F. Frolow, S. M. Franken, M. Harel, S. J. Remington, I. Silman, J. Schrag, J. L. Sussman, K. H. G. Verschueren, A. Goldman, *Protein Eng. Des. Sel.* **1992**, *5*, 197–211.
[31] J. D. Schrag M. Cygler, *Methods Enzymol.* **1997**, *284*, 85–107.
[32] P. Heikinheimo, A. Goldman, C. Jeffries, D. L. Ollis, *Structure* **1999**, *7*, R141–R146.
[33] M. Nardini B. W. Dijkstra, *Curr. Opin. Struct. Biol.* **1999**, *9*, 732–737.
[34] F. Haeffner, T. Norin, K. Hult, *Biophys. J.* **1998**, *74*, 1251–1262.
[35] P. Trodler J. Pleiss, *BMC Struct. Biol.* **2008**, *8:9*.
[36] M. Hashida, Y. Takamura, O. Kirk, T. Halkier, S. Pedersen, S. A. Patkar, M. T. Hansen, *Lipases from Hyphozyma*, Patent WO93/24619.
[37] J. D. Bendtsen, H. Nielsen, G. von Heijne, S. Brunak, *J. Mol. Biol.* **2004**, *340*, 783–795.
[38] A. Hjorth, F. Carriere, C. Cudrey, H. Woldike, E. Boel, D. M. Lawson, F. Ferrato, C. Cambillau, G. G. Dodson, L. Thim, R. Verger, *Biochemistry* **1993**, *32*, 4702–4707.
[39] F. Secundo, G. Carrea, C. Tarabiono, P. Gatti-Lafranconi, S. Brocca, M. Lotti, K. E. Jaeger, M. Puls, T. Eggert, *J. Mol. Catal. B* **2006**, *39*, 166–170.
[40] R. Higuchi, B. Krummel, R. K. Saiki, *Nucleic Acids Res.* **1988**, *16*, 7351–7367.
[41] B. Huge-Jensen, F. Andreasen, T. Christensen, M. Christensen, L. Thim, E. Boel, *Lipids* **1989**, *24*, 781–785.
[42] K. Blank, J. Morfill, H. Gumpp, H. E. Gaub, *J. Biotechnol.* **2006**, *125*, 474–483.
[43] E. Henke, S. Schuster, H. Yang, U. T. Bornscheuer, *Monatsh. Chem.* **2000**, *131*, 633–638.
[44] A. L. Ong, A. H. Kamaruddin, S. Bhatia, W. S. Long, S. T. Lim, R. Kumari, *Enzyme Microb. Technol.* **2006**, *39*, 924–929.
[45] A. L. Ong, A. H. Kamaruddin, S. Bhatia, *Process Biochem.* **2005**, *40*, 3526–3535.
[46] A. Svendsen, I. G. Clausen, S. A. Patkar, K. Borch, M. Thellersen, *Methods Enzymol.* **1997**, *284*, 317–340.
[47] J. C. Phillips, R. Braun, W. Wang, J. Gumbart, E. Tajkhorshid, E. Villa, C. Chipot, R. D. Skeel, L. Kale, K. Schulten, *J. Comput. Chem.* **2005**, *26*, 1781–1802.
[48] H. J. C. Berendsen, J. P. M. Postma, W. F. Vangunsteren, A. Dinola, J. R. Haak, *J. Chem. Phys.* **1984**, *81*, 3684–3690.
[49] J.-P. Ryckaert, G. Ciccotti, H. J. C. Berendsen, *J. Comput. Phys.* **1977**, *23*, 327–341.
[50] T. Christensen, H. Woeldike, E. Boel, S. B. Mortensen, K. Hjortshoej, L. Thim, M. T. Hansen, *Nat. Biotechnol.* **1988**, *6*, 1419–1422.

Received: October 7, 2008
Published online on January 20, 2009

